Quantum and Classical Fall of a Charged Particle onto a Stationary Dipolar Target†

E. I. Dashevskaya,‡,§ I. Litvin,‡,§ E. E. Nikitin,‡,§ and J. Troe*,§,||

Schulich Faculty of Chemistry, Technion—Israel Institute of Technology, Haifa 32000, Israel, Max-Planck-Institut für Biophysikalische Chemie, Am Fassberg 11, Göttingen D-37077 Germany, and Institut für Physikalische Chemie, Universität Göttingen, Tammannstrasse 6, Göttingen D-37077, Germany

Received: February 19, 2009; Revised Manuscript Received: March 24, 2009

The quantum dynamics of the fall of a charged particle (i.e., the capture of a charged particle) onto a stationary dipolar target is considered. Extending previous approaches for the calculation of rate coefficients in the lowest channels, we now determine rate coefficients for all channels until the quantum rate coefficients converge to their classical counterpart. The results bridge the gap between the capture of light particles (electrons) and heavy particles (ions) in the limit of sudden dynamics, when the collision time is short in comparison to the rotational period of the molecular target. The quantum-classical correspondence is discussed in terms of semiclassical numbers of channels which are open for capture in effective potentials formed by charge−dipole attraction and centrifugal repulsion. The quantum capture rate coefficients are presented through classical rate coefficients and correction factors that converge to unity for high temperatures and whose behavior at ultralow temperatures, for not too small values of the dipole moment, is determined by semiclassical numbers of capture channels.

1. Introduction

The fall of a particle onto an attractive center is one of the standard problems treated within classical as well as quantum mechanics (see, e.g., ref 1, section 14, and ref 2, sections 18 and 35). The process is characterized by capture cross sections or rate coefficients which correspond to a close approach of the attractive center by the particle. The quantum calculation of the capture cross section is based on the solution of a set of radial wave equations that describe the approach of the center accompanied by transitions between states of different relative angular momenta. These equations represent a simplified case of the more general problem of complex formation in collisions of ions or electrons with molecular targets such as described by the equations for inelastic scattering between the collisional partners with standard boundary conditions at large separations, and absorbing conditions on the surface of the complex.[3−6] The simplification arises from the approximation that all internal degrees of freedom of the target are disregarded and its orientation in space is assumed fixed. In collision theory, the latter assumption is known as the sudden approximation. It is valid when the characteristic collision time is short compared to the period of rotation of the target. This approximation constitutes an important limiting case of inelastic and reactive scattering, and it is the issue of the present article.

If the potential U determining the motion of the particle is spherically symmetric, i.e., $U = U(R)$, the calculation of the capture cross section is straightforward, both in classical and quantum mechanics (R denotes the center-of-mass distance between the collision partners). The calculation is facilitated by the conservation of the vectorial integral of motion, the orbital angular momentum, which gives rise to two exact quantum numbers, $\boldsymbol{l}$ and m. The capture problem becomes one-dimensional, and the fall is assumed to occur once a particle traverses centrifugal barriers which are formed by the superposition of the attractive potential and repulsive centrifugal interactions. If the potential is anisotropic, such that it depends also on the polar and azimuthal angles of the incoming particle in a body-fixed frame attached to the target, $U = U(R, \gamma, \phi)$, the capture dynamics is fully three-dimensional and therefore more complicated. However, if the potential is axially symmetric, $U = U(R, \gamma)$, there exists a scalar integral of motion, i.e., the projection of the orbital angular momentum onto the symmetry axis, m, and the capture dynamics becomes two-dimensional. It becomes even simpler when the anisotropic part of the potential turns out to be proportional to R^{-2}. Then it can be combined with the rotational kinetic energy to form an expression that serves as an additional integral of motion. This integral of motion, specified by two quantum numbers n and m, can be used to construct a set of one-dimensional radial equations which is formally similar to that for isotropic capture. A potential that satisfies the above condition is the charge-permanent dipole interaction superimposed on an arbitrary isotropic potential. When the latter is an isotropic charge-induced dipole interaction, one arrives at the problem of the fall of a charged particle onto a polarizable stationary dipolar target. The problem then is a simplified case of the capture of a charged particle by a neutral target with a long-range interaction which falls off as R^{-2} and R^{-4}. What is missing in this model is the charge−quadrupole interaction and the anisotropic part of the polarization interaction. As a reward for the simplification, one can apply analytical treatments at least for some parts of the problem. The considered model was used as an important limiting case in the capture of ions by molecules,[7−9] and it represents the basis for one of the approaches to the attachment of electrons to molecules, the so-called extended Vogt−Wannier model.[10,11]

The purpose of the present article is the study of the full quantum capture dynamics of the fall of a charged particle onto a stationary dipolar target, with the aim to go beyond the low-energy approximation for s-wave capture elaborated by Fabrikant and Hotop.[10,11] We include higher-order waves into the

† Part of the "Vincenzo Aquilanti Festschrift".
‡ Technion—Israel Institute of Technology.
§ Max-Planck-Institut für Biophysikalische Chemie.
|| Universität Göttingen.

10.1021/jp901515e
Published on Web 06/11/2009

capture cross sections and rate coefficients and compare the latter with their classical counterparts. This goal was already partly achieved in ref 12 when we suggested an analytical approximation for the rate coefficients that interpolates between accurate *s*-wave capture rate coefficients and all-wave capture rate coefficients for dipoleless molecules such as treated earlier.[13] Our interest in more accurate treatments is also raised by the observation[13] that the energy-dependent rate coefficients very rapidly attain their classical limit, and the temperature-dependent rate coefficients (i.e., the energy-dependent rate coefficients averaged over a thermal distribution of collision energies) virtually coincide with the classical Langevin rate coefficient (in a R^{-4} potential) for temperatures at which the *p*-wave capture becomes classically open. This seemingly weak quantum effect in the rate coefficients was interpreted in ref 13 as the consequence of strong compensating quantum effects such as tunneling and overbarrier reflection. As a result, it became possible to design a simple analytical expression for the rate coefficients from zero to high temperatures. In the present article we address a similar question for sudden dynamics of capture in the field of a stationary polarizable dipole. Correspondingly, our plan is the following. In section 2 we briefly review the theory of the quantum fall in the field of the considered potential. Section 3 presents the results of numerical calculations of capture probabilities and rate coefficients. Section 4 describes the classical theory of capture and provides analytical expressions for the rate coefficients. In section 5 we present a comparison of quantum capture rate coefficients with their classical counterparts. Section 6 concludes the article.

2. Quantum Description of Capture Dynamics

The potential of a charged particle in the field of a stationary polarizable dipole is given by

$$U(R,\gamma) = -q\mu_D \cos\gamma/R^2 - q^2\alpha/2R^4 \quad (1)$$

where R is the center-of-mass distance between the charged particle and the neutral dipolar target, μ_D is the dipole moment and α the polarizability of the target, q is the charge of the incoming particle, and γ is the angle between the dipole axis **d** and the collision axis **R**. If the vector **d** defines the polar axis for the incoming particle, which is possible for a stationary dipole, i.e., in a space-fixed coordinate system, the Hamiltonian of the particle becomes

$$\hat{H} = -\frac{\hbar^2 d^2}{2\mu d R^2} + \frac{\hat{\mathbf{L}}^2(\gamma,\phi)}{2\mu R^2} + U(R,\gamma) \quad (2)$$

where $\hat{\mathbf{L}}$ is the operator of the orbital angular momentum and μ is the reduced mass of the system. When the charge−dipole term in eq 1 is combined with the centrifugal term in eq 2, one can rewrite the expression for $\hat{H}$ as

$$\hat{H} = -\frac{\hbar^2 d^2}{2\mu d R^2} + \frac{\hat{V}(\gamma,\phi)}{2\mu R^2} - \frac{q^2\alpha}{2R^4} \quad (3)$$

where $\hat{V} = \hat{\mathbf{L}}^2 - 2q\mu_D\mu\cos\gamma$. Since $\hat{V}$ commutes with $\hat{H}$, the operator $\hat{V}$ can be replaced by the set of its eigenvalues V_v. This has the result that the three-dimensional Hamiltonian $\hat{H}(R,\gamma,\phi)$ is reduced to a set of uncoupled one-dimensional Hamiltonians $\hat{H}_v(R)$, provided that **d** is chosen as the quantization axis for the orbital angular momentum. As a result the wave equation assumes the form[10,11]

$$\left\{-\frac{\hbar^2 d^2}{2\mu d R^2} + \frac{V_v}{2\mu R^2} - \frac{q^2\alpha}{2R^4}\right\}\psi_{E,v}(R,D) = E\psi_{E,v}(R,D) \quad (4)$$

The solution of this equation, with an absorbing boundary condition at small values of R (incoming and outgoing waves at large R and only incoming waves at small R), yields the capture probabilities $P_v(E)$ which in turn determine the integral capture cross section

$$\sigma(E) = \frac{\pi\hbar^2}{\mu E}\sum_v P_v(E) \quad (5)$$

In what follows we use the scaled quantities introduced in ref 13, i.e., the distance ρ and the energy ε where $\rho = R/R_L$ and $\varepsilon = (\mu R_L^2/\hbar^2)E$ with $R_L = (\mu q^2\alpha)^{1/2}/\hbar$. Using these variables, eq 4 assumes the form

$$\left\{-\frac{d^2}{2d\rho^2} + \frac{v_v}{2\rho^2} - \frac{1}{2\rho^4}\right\}\psi_{\varepsilon,v}(\rho) = \varepsilon\psi_{\varepsilon,v}(\rho) \quad (6)$$

Here, v_v are successive eigenvalues of the operator $\hat{\boldsymbol{v}} = \hat{\mathbf{l}}^2 - 2d\cos\gamma$, with $\hat{\mathbf{l}}^2 = \hat{\mathbf{L}}^2/\hbar^2$ and $d = q\mu\mu_D/\hbar^2$. The eigenvalues $v_v = v_v(d)$ can be specified by two indices, m, corresponding to the conserved projection of the relative angular momentum onto the vector **d**, and n, successively enumerating eigenvalues for a given m. For convenience, we can assume that n takes the values $n = |m|, |m+1|, |m+1|, \ldots$. Note that the eigenvalues $v_{n,m}$ with $m = 0$ are nondegenerate, and those with $|m| > 0$ are doubly degenerate. Absorbing the subscripts n, m into the variable parameter v, we rewrite the capture eq 6 as

$$\left\{-\frac{d^2}{2d\rho^2} + \frac{v}{2\rho^2} - \frac{1}{2\rho^4}\right\}\psi_\varepsilon(\rho,v) = \varepsilon\psi_\varepsilon(\rho,v) \quad (7)$$

where v assumes any values from the set $v_{n,m}(d)$. The solutions of eq 7 give the capture probabilities $P(\varepsilon, v)$ which generate the probabilities of capture in the n, m channel as

$$P_{n,m}(\varepsilon,d) = P(\varepsilon,v)|_{v=v_{n,m}(d)} \quad (8)$$

In turn, $P_{n,m}(\varepsilon, d)$ define the integral capture cross sections and the energy-dependent rate coefficients. A scaled version of the latter, $\chi(\varepsilon, d)$, i.e., the ratio of the energy-dependent rate coefficient $k(E)$ and the energy-independent Langevin rate coefficient $k^L = 2\pi q(\alpha/\mu)^{1/2}$, is given by

$$\chi(\varepsilon,d) = \sum_{m=-\infty}^{m=\infty}\sum_{n=|m|}^{n=\infty}\chi_{n,m}(\varepsilon,d);$$
$$\chi_{n,m}(\varepsilon,d) = P_{n,m}(\varepsilon,d)/2\sqrt{2\varepsilon} \quad (9)$$

The form of the effective potential in eq 7 shows that capture occurs as a result of entering the region of high attraction across

the potential step for $v < 0$, while for $v > 0$ it occurs as a result of crossing a barrier of the height $\delta = v^2/8$.

For $d = 0$, the eigenvalues of $\hat{v}$ are $v_{n,m}|_{d=0} = n(n+1)$, such that eq 7 can be rewritten as

$$\left\{-\frac{d^2}{2d\rho^2} + \frac{l(l+1)}{2\rho^2} - \frac{1}{2\rho^4}\right\}\psi_{\varepsilon,l}(\rho) = \varepsilon\psi_{\varepsilon,l}(\rho) \qquad (10)$$

with the understanding that the eigenvalue $l(l+1)$ repeats $2l+1$ times, and l assumes the values $l = 0, 1, 2, \ldots$. Then eq 9 can be represented as

$$\chi(\varepsilon, d)|_{d=0} \equiv \chi(\varepsilon) = \sum_{l=0}^{l=\infty}(2l+1)\chi_l(\varepsilon); \quad \chi_l(\varepsilon) = P_l(\varepsilon)/2\sqrt{2\varepsilon} \qquad (11)$$

where $P_l(\varepsilon)$ is the capture probability for the radial eq 10. Obviously, eqs 10 and 11 are the standard equations for capture in an isotropic potential $-1/2\rho^4$, yielding asymptotically the Langevin (L) and Vogt−Wannier (VW) limits, $\chi(\varepsilon)|_{\varepsilon\gg1} = \chi^{L} = 1$ and $\chi(\varepsilon)|_{\varepsilon\to0} = \chi^{VW} = 2$. Formally, eq 10 is similar to eq 6; however, the essential difference is that the long-range interaction in eq 10 is attractive only for $l = 0$ with ρ^{-4} asymptotic behavior, while there are a finite number of attractive terms with ρ^{-2} asymptotic behavior in eq 6.

Once the $\chi_{n,m}(\varepsilon, d)$ are found, they directly define the partial and total thermally averaged rate coefficients, $\bar{\chi}_{n,m}(\theta, d)$ and $\bar{\chi}(\theta, d)$

$$\bar{\chi}_{n,m}(\theta, d) = \int_0^\infty \chi_{n,m}(\varepsilon, d) \times \sqrt{2/\pi\theta^3}\exp(-\varepsilon/\theta)\sqrt{2\varepsilon}\,d\varepsilon$$
$$\bar{\chi}(\theta, d) = \sum_{m=-\infty}^{m=\infty}\sum_{n=|m|}^{n=\infty}\bar{\chi}_{n,m}(\theta, d) \qquad (12)$$

where the second factor in the integrand is the Maxwell−Boltzmann distribution that contains a reduced temperature θ:

$$\theta = (\mu R_L^2 k_B/\hbar^2)T = (q^2\alpha\mu^2 k_B/\hbar^4)T \qquad (13)$$

The calculation of capture probabilities $P_{n,m}(\varepsilon, d)$ is straightforward once the eigenvalues $v_{n,m}(d)$ are known. As mentioned in ref 12, they coincide, though in a different parametrization, with the eigenvalues of a rigid dipolar rotor in a uniform electric field. These eigenvalues were used for the calculation of adiabatic channel potentials for the capture of dipolar rotors by ions,[14,15] and they are available in analytical approximation for a wide range of the parameters.[16,17] For small enough d, the $v_{n,m}$ can be calculated by a second-order perturbation approach with the result

$$v_{n,m}(d)|_{n=l} = l(l+1) - \frac{d^2}{2}\left(\frac{3m^2 - l(l+1)}{l(l+1)(2l-1)(2l+3)}\right) \qquad (14)$$

and $v_{0,0} = -(2/3)d^2$. We note in passing that the latter result for charge−dipole interaction corresponds to the second-order perturbation treatment on the basis of free radial s- and p-wave motion of the incoming particle. Within the same approach, one can estimate the second-order effect for the charge−quadrupole interaction which yields a term proportional to R^{-4} in the interaction potential and for the anisotropy of the charge-induced dipole interaction.

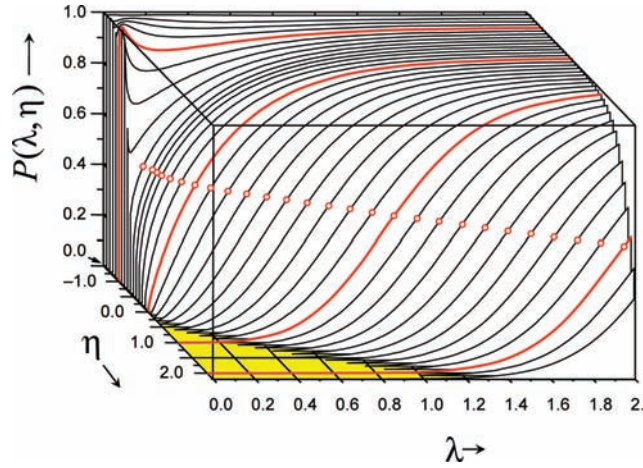

Figure 1. Capture probabilities $P = P(\lambda, \eta)$ (see text; the heavy lines correspond to $\eta = -1, 0, 1, 2$; for $\eta = 0, 1, 2$, they correspond to the capture probabilities for a dipoleless target with $l = 0, 1, 2$; the open symbols mark the positions where $P = 1/2$).

3. Quantum Capture Probabilities and Rate Coefficients

The capture probabilities $P(\varepsilon, v)$, found by numerical solution of eq 7, are represented in Figure 1 in the form of $P(\lambda, \eta)$ as a function of the variables $\lambda(\varepsilon)$ and $\eta(v)$ given by

$$\lambda(\varepsilon) = \sqrt{(1/4) + 2\sqrt{2\varepsilon}} - 1/2, \quad \eta(v) = \sqrt{(1/4) + v} - 1/2 \qquad (15)$$

In these variables, $\lambda(\varepsilon)$ equals l each time when the energy ε coincides with the height $(l(l+1))^2/8$ of the reduced centrifugal barrier of the effective potential in eq 10 for $l > 0$, and $\eta(v)$ equals l each time when v coincides with $l(l+1)$, i.e., the eigenvalues of v for $d = 0$. The probabilities $P_l(\varepsilon)$ are drawn as graphs in the planar sections specified by the points $\eta(v) = l$; the marked points $\lambda(\varepsilon) = l$ indicate the position where $P_l(\varepsilon) = 1/2$. Note that according to eq 15 the variable η is real only for $v \geq -1/4$. For $v \leq -1/4$, it can be redefined to make it real also. If one puts $\eta(v) = -\mathrm{Im}\{[(1/4) + v]^{1/2}\} - 1/2$ for $v \leq -1/4$, then one will have a single continuous variable $\eta(v)$ that corresponds to any value of v and which equals $-1/2$ for $v = -1/4$. The significance of this point is seen in the analytical perturbation expression (valid for small ε and λ) for $P(\varepsilon, v)$ (see refs 10 and 11) which shows that, for $\eta > -1/2$, the capture probability disappears as $\varepsilon^{\eta+1/2}$, while, for $\eta < -1/2$, at $\varepsilon = 0$ it starts from nonzero values. For $\eta = 0$, this energy dependence conforms with Bethe's law[18] for s-wave capture, and, for $\eta = l$, $l > 0$, it corresponds to Wigner's law[19] for capture with higher angular momenta.

The rather simple structure of $P(\lambda, \eta)$ in the following will be used for the analysis of the d-dependence of the capture probabilities $P_{n,m}(d)$. For $d = 0$, there exist only curves $P_l(\lambda)$ in the sections $\eta = l$, $l = 0, 1, 2, \ldots$. These are the probabilities of capture by a dipoleless polarizable target.[13] Analytical approximations valid over a wide range of ε are available for $l = 0, 1, 2, 3, 4$; see ref 12. With small nonzero d, each curve $P_l(\lambda)$ splits into $l+1$ components $P_{n,m}(\lambda)$ where n assumes the same value as l, and $m = 0, \pm 1, \ldots, \pm l$. With increasing d, the components $P_{n,m}(\lambda)$, which are shifted to the left of $P_l(\lambda)$, move

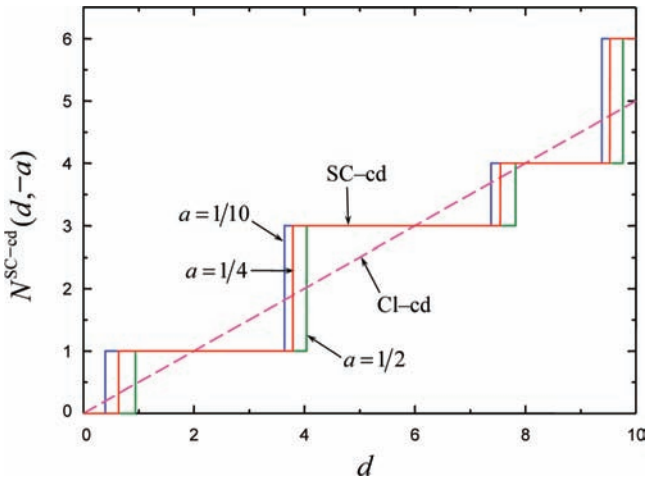

Figure 2. Number of eigenvalues $N^{SC-cd}(d, a)$ of the matrix $v(d)$ which are below the parameter $-a$ that conventionally defines a cd semiclassical channel as an open one (the straight dashed line corresponds to the classical number of attractive cd states; see section 5).

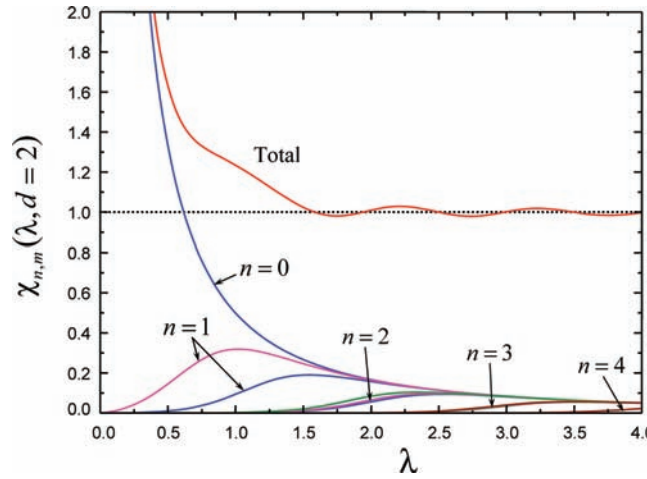

Figure 3. Quantum energy-dependent reduced capture rate coefficients $\chi(\lambda, d)$ and their partial contributions $\chi_{n,m}(\lambda, d)$ for $d = 2$. Each n-manifold encompasses curves with $|m| = 0,1,..., n$ (the dotted horizontal line corresponds to the Langevin limit).

further in the direction of negative values of η. The curves $P_{n,m}(\lambda)$, to the left from the section plane $\eta = -1/2$, show a nonmonotonic dependence on λ (or ε) in their trend to the high-energy asymptotics $P_{n,m}(\lambda)_{\lambda \gg 1} \rightarrow 1$. This behavior can be interpreted as the result of a reflection of the incoming wave, entering through the strongly attractive R^{-2} potential, by the additional drop of the potential from the R^{-4} interaction. The probabilities, which correspond to large negative values of v, eventually cluster at the left-hand side of the box shown in Figure 1. They assume the shape of step functions, $P_{n,m}(\lambda) \rightarrow \Theta(\lambda)$. This is the classical probability of capture in the field of purely attractive charge−dipole (cd) effective potentials which are proportional to R^{-2}. One can conveniently define the semiclassical number of capture channels $N^{SC-cd}(d)$ for this type of interaction as the number of the eigenvalues of v that do not exceed a certain negative value $-a$, presumably being close to $-1/4$. If one puts the respective capture probabilities equal to unity and neglects the capture in all other channels (being not purely repulsive), with the help of eq 9 one obtains an estimate of the SC-cd rate coefficient for capture through these channels, i.e.

$$\bar{\chi}^{SC-cd}(\theta, N^{SC-cd}) = N^{SC-cd}(d, a)/\sqrt{2\pi\theta} \qquad (16)$$

The dependence of $N^{SC-cd}(d, a)$ on d, for various values of a, is shown in Figure 2. The increments of $N^{SC-cd}(d, a)$ are either 1 or 2, depending on the value of m ($m = 0$ or $|m| > 0$) in the eigenvalue v_{nm} that just becomes less than $-a$. One also sees the sensitivity of the positions of the steps to the chosen values of a.

In the general case, the rate coefficients $\chi(\varepsilon, d)$ and $\bar{\chi}(\theta, d)$ should be calculated from numerically accurate values of the capture probabilities $P_{n,m}$. An example of the dependence of χ on λ is shown in Figure 3 together with the partial contributions $\chi_{n,m}$ for $d = 2$ when $N^{SC-cd}(d, a) = 1$. In this case, the monotonic decrease of the total energy-dependent rate coefficients is essentially determined by the contribution of four partial terms $\chi_{0,0}$, $\chi_{1,0}$, $\chi_{1,\pm1}$, while higher terms only produce undulations of $\chi(\lambda, d)$ around the classical asymptote. This behavior is qualitatively similar to the capture by nonpolar targets (see Figure 2 of ref 13). The quantitative difference is that, in the present case, the charge−dipole interaction extends into the

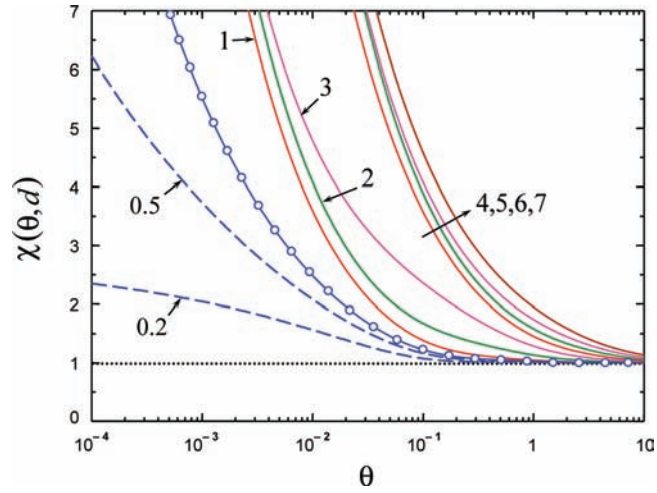

Figure 4. Quantum temperature-dependent reduced capture rate coefficients $\chi(\theta, d)$ for several values of d (see text; the circles mark the curve for the critical value of $d^* = 0.6395$ corresponding to $v = -1/4$; the dashed curves are for $d < d^*$; the full curves are for $d > d^*$; the curves are labeled by the values of d, and the dotted horizontal line indicates the Langevin limit).

energy region across which $\chi(\lambda, d)$ shows a strong decrease with increasing energy. The temperature dependence of the rate coefficients $\bar{\chi}(\theta, d)$ is presented in Figure 4 for various values of d. For d below the critical value $d^* = 0.6395$, this dependence was already discussed in detail,[12] so that we dwell here on cases with $d > d^*$. An interesting feature is the clustering of curves with $d = 1$, 2, 3 and with $d = 4$, 5, 6, 7 in the low-temperature region. This is explained by the fact that the SC-cd number of states is the same ($N^{SC-cd} = 1$ for $d = 1$, 2, 3 and $N^{SC-cd} = 3$ for $d = 4$, 5, 6, 7), while the difference between the curves within the same cluster comes from the stronger reflection of the incoming wave at the drop of the polarization superimposed on the more gradual cd attraction.

The given results allow one to check the accuracy of an approximate analytical expression for $\bar{\chi}(\theta, d)$, i.e., $\bar{\chi}^{app}(\theta, d)$, suggested in ref 12. The function $\bar{\chi}^{app}(\theta, d)$ there was expressed by the rate coefficients $\bar{\chi}(\theta) \equiv \bar{\chi}(\theta, d)|_{d=0}$, $\bar{\chi}^{min}_{0,0}(\theta) \equiv \bar{\chi}_{0,0}(\theta, d)|_{d=0}$ (the total and s-wave capture rate coefficients for a dipoleless target), $\bar{\chi}^{max}_{0,0}(\theta) \equiv \bar{\chi}^{SC-cd}(\theta, N^{SC-cd})|_{N^{SC-cd}=1} = 1/(2\pi\theta)^{1/2}$, and an additional fitting function $G(\theta, d)$ that

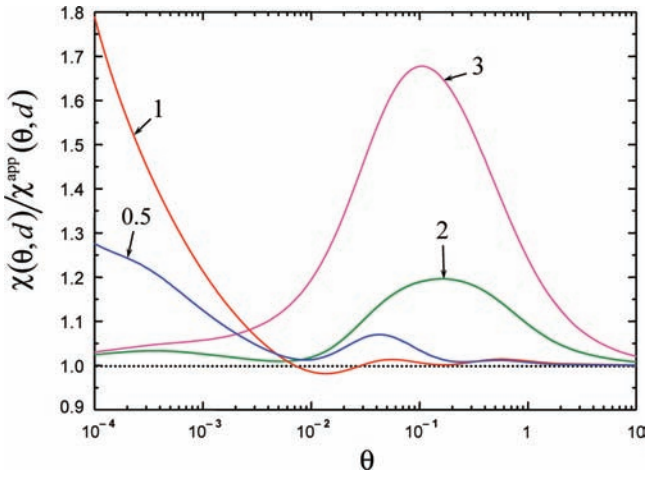

Figure 5. Comparison of accurate quantum temperature-dependent capture rate coefficients $\chi(\theta, d)$ and approximate values $\chi^{app}(\theta, d)$ given by eq 17 ($d = 0.5, 1, 2, 3$; θ is the scaled temperature; the curves are labeled by the values of d, and the dotted horizontal line is drawn for orientation).

introduces the dependence of $\bar{\chi}^{app}(\theta, d)$ on d. This approximation was of the form

$$\bar{\chi}^{app}(\theta, d) = \bar{\chi}(\theta) + [\bar{\chi}^{max}_{0,0}(\theta) - \bar{\chi}^{min}_{0,0}(\theta)] \times [1 - \exp(-G(\theta, d))] \quad (17)$$

Analytical expressions for the fitting functions entering the rhs of eq 17 were given in ref 12. The accuracy of the approximate expression for the capture rate can be judged from the ratio $\bar{\chi}(\theta, d)/\bar{\chi}^{app}(\theta, d)$ plotted in Figure 5. We see that, for $d < 1$, the accuracy of the approximation in eq 17 is better than 5% at $\theta > 0.01$, while it deteriorates rapidly with the increase of d.

4. Classical Capture Probabilities and Rate Coefficients

The classical rate coefficients for the capture in the potential in eq 1 can be calculated analytically by using the same integral of motion as in the quantum calculations.[9] The classical Hamiltonian is of the form

$$H^{Cl} = \frac{P_R^2}{2\mu} + \frac{W(P_\gamma, P_\varphi, \gamma, \phi)}{2\mu R^2} - \frac{q^2\alpha}{2R^4} \quad (18)$$

where P_R, P_γ, P_ϕ are the momenta conjugate to the coordinates R, γ, ϕ. The integral of motion $W(P_\gamma,P_\phi,\gamma,\phi) = L^2(P_\gamma,P_\phi,\gamma,\phi) - 2q\mu_D \cos\gamma$ can be expressed, with a proper change of variables, through their asymptotic values. Explicitly, taking these variables as the initial angular momentum L_i and the initial orientation angle $\cos\gamma_i$, we write $W = L_i^2 - 2q\mu_D \cos\gamma_i$. The classical capture probabilities $P^{Cl}(E, W)$, which are the counterpart of the quantum quantity $P(\varepsilon, \upsilon)$ for the Hamiltonian in eq 18, are expressed by the respective step functions $\Theta(x)$. Explicitly, one has

$$P^{Cl}(E, W) = \Theta(E - D(W)) \quad (19)$$

where $D(W)$ is the centrifugal potential barrier for the effective potential in eq 18, i.e.

$$D = W^2 \cdot \Theta(W)/8\mu^2 q^2 \alpha \quad (20)$$

Yet another step function causes the barrier height to disappear for a purely attractive effective interaction. When U and W are expressed through the variables L_i and γ_i as well as the parameter μ_D, the classical counterpart of the quantum capture probability in eq 8 can be written as

$$P^{Cl}(E, \mu_D; L_i, \gamma_i) = P^{Cl}(E, W)|_{W=W(L_i,\gamma_i,\mu_D)} \quad (21)$$

According to eq 19, the capture occurs both in asymptotically attractive ($\cos\gamma_i > 0$) and repulsive ($\cos\gamma_i < 0$) channels. The former corresponds to asymptotically attractive and repulsive effective interactions (i.e., interactions that comprise the potentials and the centrifugal energy), while the latter corresponds to repulsive interactions. In the calculation of energy-dependent and temperature-dependent classical rate coefficients χ^{Cl} and $\bar{\chi}^{Cl}$, the double summation over the quantum numbers n, m in eq 9 is replaced by a double integration over L_i and γ_i. In contrast to the reduced quantum rate coefficients which depend on two dimensionless variables (ε, d or θ, d), it turns out that the reduced classical rate coefficients depend on one dimensionless variable only,[7,8] i.e., on the classical dimensionless temperature θ^{Cl}, defined by

$$\theta^{Cl} = 2\alpha k_B T/\mu_D^2 \quad (22)$$

The explicit expression for $\bar{\chi}^{Cl}(\theta^{Cl})$, which is obtained through a straightforward integration of the probabilities from eq 19 over L_i, γ_i and the Maxwell−Boltzmann distribution, reads

$$\bar{\chi}^{Cl}(\theta^{Cl}) = \frac{1}{2\sqrt{\pi\theta^{Cl}}} + 1 + \frac{1}{2}\sqrt{\frac{\theta^{Cl}}{\pi}}(1 - \exp(-1/\theta^{Cl})) - \frac{1}{2}\mathrm{erf}(1/\sqrt{\theta^{Cl}}) \quad (23)$$

where $\mathrm{erf}(x) = (2/\sqrt{\pi})\int_0^x \exp(-t^2)\,dt$. Equation 23 conforms with the numerical results from classical trajectory calculations for ion-polarizable dipole capture in the sudden limit,[8] but it differs from the analytical expression for capture rate coefficients in the so-called ACIOS approximation (eq 28 from ref 20); note that the latter, for a charge−dipole system, is identical to the sudden approximation discussed here.[9] The difference presumably can be ascribed to neglect of the capture in ref 20 through the asymptotically repulsive cd interaction.

The two limiting expressions of $\bar{\chi}^{Cl}(\theta^{Cl})$ correspond to the classical capture by a stationary unpolarizable dipolar target ($\theta^{Cl} \ll 1$) and by a nonpolar polarizable target ($\theta^{Cl} \gg 1$):

$$\bar{\chi}^{Cl}(\theta^{Cl}) = \begin{cases} 1/2\sqrt{\pi\theta^{Cl}}, & \theta^{Cl} \ll 1 \\ 1, & \theta^{Cl} \gg 1 \end{cases} \quad (24)$$

A plot of $\bar{\chi}^{Cl}(\theta^{Cl})$ is shown in Figure 6. Also shown are the high- and low-temperature approximations to $\bar{\chi}^{Cl}(\theta^{Cl})$ such as given by eq 24. The anisotropic character of the capture can be conveniently characterized by rigidity factors[21] f_{rigid}, i.e., the ratio of the capture rate coefficients to their counterparts within the so-called locked-dipole model or the phase-space theory (PST) when the orientation of the dipole is assumed to be directed

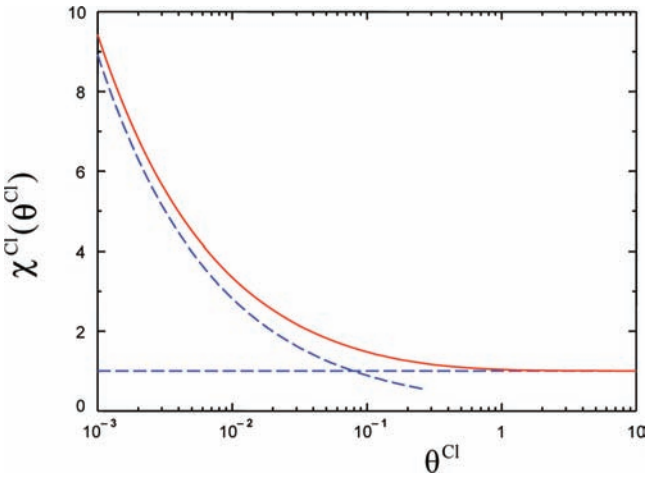

Figure 6. Classical reduced rate coefficients χ^{Cl} as a function of the reduced temperature θ^{Cl} (full line, see eq 23; the dashed lines correspond to the low- and high-temperature approximations given by eq 24).

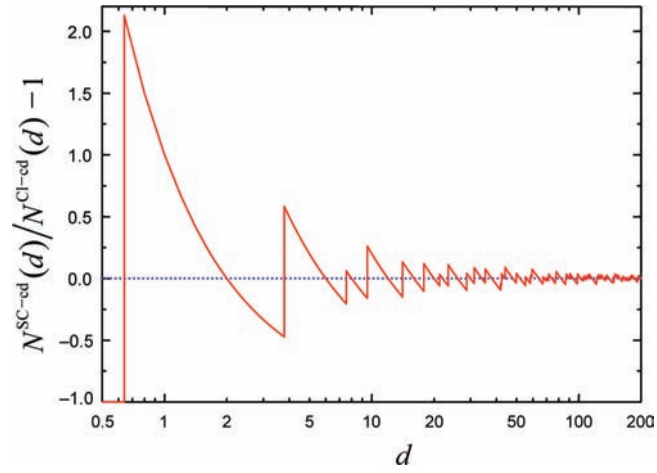

Figure 7. Convergence of the semiclassical numbers of capture channels $N^{SC-cd}(d, a)$ to their classical counterparts $N^{Cl-cd}(d)$ for $a = 1/4$ (the figure shows the relative deviation,; the dotted horizontal line is drawn for orientation).

along the collision axis. In our case, the sudden rigidity factor f_{rigid}^{sudd} is equal to the ratio of $\bar{\chi}^{Cl}(\theta^{Cl})$ from eq 23 and $\bar{\chi}_{PST}^{Cl} = 1 + 2/(\pi\theta^{Cl})^{1/2}$. The high- and low-temperature asymptotic values of f_{rigid}^{sudd} are 1 and 1/4. The former value reflects the vanishing effect of the anisotropy at high temperatures, while the latter illustrates the average value of the projection of the unit dipole moment onto the collision axis over the attractive collision hemisphere with $\cos\gamma_i \geq 0$ (see also section 6).

5. Comparison of Quantum and Classical Rate Coefficients

The comparison of classical and quantum rate coefficients can be accomplished once θ^{Cl} is related to θ. From eq 13 and 22 we obtain

$$\theta^{Cl} = 2\theta/d^2 \tag{25}$$

so that, for the same variable θ and different values of d, one can directly compare the two reduced rate coefficients, $\bar{\chi}(\theta, d)$ and $\bar{\chi}^{Cl}(2\theta/d^2)$. It is clear that $\bar{\chi}(\theta, d)$ will approach $\bar{\chi}^{Cl}(2\theta/d^2)$ at high temperatures. We first concentrate on low temperatures where the classical rate coefficients are given by their low-temperature limit corresponding to cd capture (see eq 24)

$$\bar{\chi}^{Cl-cd}(\theta, d) = d/2\sqrt{2\pi\theta} \tag{26}$$

The low-temperature classical approximation is valid when the number of channels, which are open for capture through the charge−dipole interaction, is large. Comparing eq 26 with eq 16, one sees that the factor $d/2$ in eq 26 should be regarded as the classical counterpart of the SC number of states, i.e., $d/2 = N^{Cl-cd}(d)$. Figure 7, showing the relative deviation $\Delta_N(d) = (N^{SC-cd} - N^{Cl-cd})/N^{Cl-cd}$, demonstrates how the SC number of states $N^{SC-cd}(d)$ converges to $N^{Cl-cd}(d)$.

In the general case, when N is not large and the polarization interaction is not neglected, the comparison can be accomplished through the numerically calculated quantum rates and their classical counterparts given by the analytical expressions.[23] Figure 8 shows such a comparison for different values of d, which correspond to qualitatively different relations between N^{SC-cd} and N^{Cl-cd} with $a = 1/4$: $N^{SC-cd} = 0$ for $d < d^*$, $N^{SC-cd} > N^{Cl-cd}$ for $d = 1$ and 4, $N^{SC-cd} \approx N^{Cl-cd}$ for $d = 2$ and 6, and $N^{SC-cd} < N^{Cl-cd}$ for $d = 3$ and 7 (compare Figures 2 and 7). We first note that the low-temperature dependence of $\bar{\chi}(\theta, d))$ is determined by the low-energy dependence of $\chi(\varepsilon, d)$ (see section 3), and therefore $\bar{\chi}(\theta, d))$ diverges as $T^{-1/2}$ for $\eta < -1/2$ and as T^{η} for $-1/2 \leq \eta < 0$. Since the classical rate $\bar{\chi}^{Cl}(\theta, d))$ diverges as $T^{-1/2}$, it is convenient to compare quantum and classical rate coefficients in terms of the correction function $C(\theta,d) = \bar{\chi}(\theta,d)/\bar{\chi}^{Cl}(2\theta/d^2)$. One sees from Figure 8 that the convergence of $C(\theta, d)$ with increasing θ to its asymptotic value $C(\theta, d)|_{\theta\gg1} \to 1$, depending on d, occurs from different sides of the horizontal dotted line $C = 1$. This behavior of $C(\theta, d)$ can be rationalized by the observation that, for $\theta \to 0$, there are three different types of the limits of $C(\theta,d)|_{\theta\ll1}$: for $0 < d < d^*$, $C(\theta, d) \to 0$ as $\theta^{1/2+\eta}$, $-1/2 < \eta < 0$ (Fabrikant−Hotop limit); for $d = 0$, $C(\theta, d)|_{d=0} \to 2$ (Vogt−Wannier limit); for $d > 1$, $C(\theta, d) \to N^{SC-cd}/N^{Cl-cd} = 2N^{SC-cd}(d)/d$ (semiclassical limit).

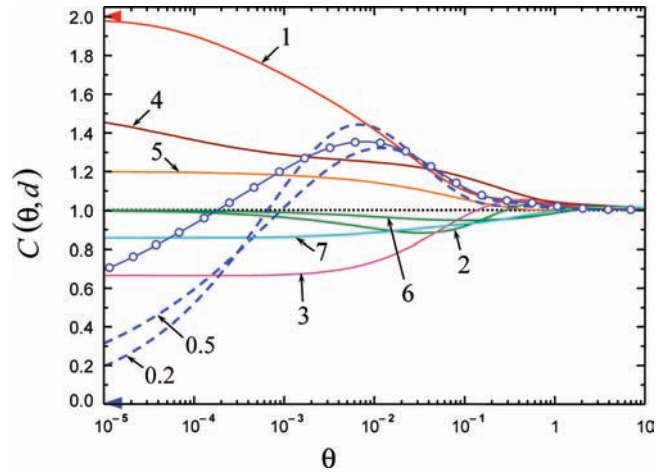

Figure 8. Correction factor $C(\theta, d)$ to the classical rate coefficient (see text, the symbols mark the critical value of $d^* = 0.6395$ corresponding to $v = -1/4$, the dashed curves are for $d < d^*$, and the full curves are for $d > d^*$; the filled symbols at the ordinate axis mark the Fabrikant−Hotop and Vogt−Wannier limits for small nonzero and zero values of d, respectively; the curves are labeled by the values of d, and the dotted horizontal line indicates the classical limit).

The existence of two different limits for $d < d^*$, for very small nonzero value of d and for $d = 0$, predicts a nonmonotonic dependence of $C(\theta, d)$ on θ which is explained by the interplay between capture induced by the polarization and charge−dipole forces. With decreasing θ, $C(\theta, d)$ first increases, as it should

when the capture occurs in the quantum regime for a $-1/R^4$ potential, and then decreases, partly quenching the classical $\theta^{-1/2}$ divergence in the quantum regime of capture for the $-1/R^2$ potential. As seen from Figure 6, the effect of the cd interaction begins to show up at about $\theta^{Cl} \approx 0.1$, the crossing point between the dotted curves corresponding to the high- and low-temperature approximations for $\chi^{Cl}(\theta^{Cl})$. Considering the relation between θ^{Cl} and θ as given by eq 25, we therefore expect that the effect of the cd interaction, which manifests itself in the decrease $C(\theta, d)$ with decreasing θ, will show up below $\theta \approx d^2/10$. This feature is illustrated by the graphs of $C(\theta, d)$ for $d = 0.5$ and $d = 0.2$. For very small d, the function $C(\theta, d)$ increases with decreasing the temperature, being approximately equal to $\bar{\chi}(\theta)$ and as if tending to the Vogt−Wannier limit 2, and then sharply drops to the Fabrikant−Hotop limit zero at zero temperature across the narrow temperature range of about $d^2/10$.

For $d > d^*$, the behavior of $C(\theta, d)$ is almost monotonic as a function of θ and nonmonotonic as a function of d. The latter feature is related to the fact that the ratio N^{SC-cd}/N^{Cl-cd} is an undulating function of d; see Figure 7. Interestingly, the zero-temperature semiclassical limit (arrows at the ordinate axis) is approached already for $d = 1$, when only one cd classical capture channel is open. Small deviations of the low-temperature portions of the graphs from the zero-temperature limits indicate a weak effect of the polarization interaction which, in principle, could be expected to manifest itself as a partial reflection of the incoming wave from the additional drop of the R^{-4} potential on the background of the much smoother R^{-2} interaction potential. On the whole, one observes an increasing approach of the curves with $d = 1-7$ to the horizontal line (classical limit) when d increases. The rather small deviation of the curves $C(\theta, d)$ from unity for $d = 2$ and $d = 6$ across a very wide temperature range is the consequence of the fact that, for these values of d, the adiabatic channel cd and the classical cd number of states are accidentally nearly equal to each other.

6. Conclusions

By extending the interaction potential to that of stationary dipolar polarizable targets, the present work generalizes our previous study[13] of the quantum fall (capture) of charged particles onto nonpolar polarizable targets. The calculation of energy- and temperature-dependent capture rate coefficients is then one of the simplest within the treatments of the capture in anisotropic interactions since here exists an extra integral of motion that considerably facilitates the computations. As in ref 13, we have found a fast convergence with increasing temperature of the quantum rate coefficients to their classical counterparts. This is the result of a "smoothing" of the discrete partial rate coefficients that is caused by large quantum corrections in crossing the centrifugal barriers, by the splitting of the barriers by the charge−dipole interaction, and by the absence of wave reflection at the drop of the attractive effective (charge−dipole plus centrifugal) potentials that are proportional to R^{-2}.

The capture by a stationary target with an anisotropic interaction is equivalent to the sudden approximation in collision theory, such that the results of this work are quite generally applicable to the calculation of complex formation rates in collisions of charged particles (electrons or ions) with slowly rotating molecules. In a translationally and rotationally canonical ensemble of charged particles and polarizable dipolar molecules, the capture regime with respect to rotationally inelastic events en route to complex formation is controlled by the value of an appropriate Massey parameter ξ, the ratio of the mean collision time to the mean rotational period.[8] In the spirit of the discussion in ref 8 and in connection with eqs 2.11−2.14 of ref 8 as applied to diatomic molecules, we write the Massey parameter here as

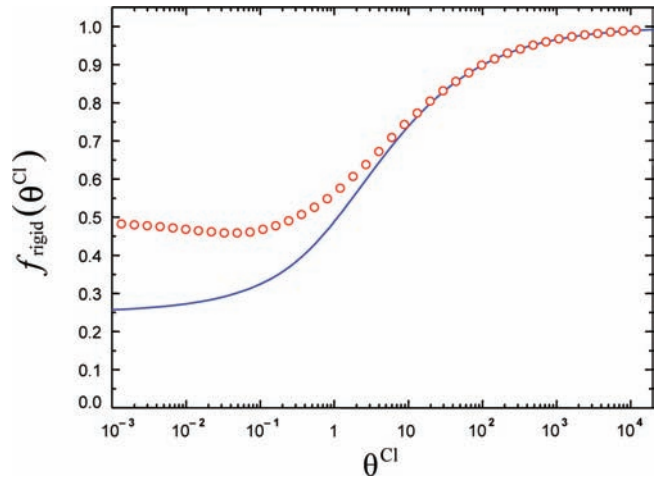

Figure 9. Comparison of the rigidity factors $f_{rigid}(\theta^{Cl})$ for sudden (full curves) and adiabatic (open circles) dynamics as a function of the reduced temperature θ^{Cl}, for the classical capture of a charged particle by a dipolar polarizable target.

$$\xi = \frac{1}{\pi}\sqrt{B/k_B T}\,\sqrt{d} \tag{27}$$

where B is the rotational constant of the diatom (in energy units; for polyatomic molecules, B should be replaced by a certain mean of rotational constants). The sudden regime corresponds to the condition $\xi \ll 1$, while the reverse condition, $\xi \gg 1$, determines the adiabatic regime when a molecule rotates fast about the collision axis. In both limiting cases, one can use simplified treatments of the capture, considering either the capture by a stationary target (the sudden case) or by a target whose projection of the intrinsic angular momentum (i.e., the rotational orientation) follows the collision axis (the adiabatic case). Intermediate cases between sudden and adiabatic dynamics present a complicated problem that requires extensive numerical calculations within standard molecular collision theory.

When d is of the order of unity or slightly larger, which is the case for the capture of electrons by molecules, the sudden limit is reached when the condition $T \gg B/k_B$ is fulfilled. For heavy molecules (for which B/k_B is of the order of fractions of kelvins), therefore, most temperatures of practical interest correspond to the sudden limit, provided that the capture can still be considered independent of other inelastic events. For the capture of muons or ions, d, which is proportional to the reduced mass of the colliding partners, is normally much larger than unity. Then, the sudden limit is attained at considerably higher temperatures, tens of kelvins for muons and hundreds of Kelvins for ions. Below this range the adiabatic description of the dynamics is more appropriate. Under the condition of classical motion of the partners, the transition from adiabatic to sudden dynamics was investigated in ref 8. The rate coefficients in the intermediate regime can conveniently be represented by rigidity factor f_{rigid} which depends on ξ; see refs 8, 15, and 22−25. It was shown (see, e.g., ref 25) that the values of f_{rigid} are between those for adiabatic and sudden limits, $f_{rigid}^{sudd} \le f_{rigid} \le f_{rigid}^{adia}$, such that two quantities, f_{rigid}^{sudd} and f_{rigid}^{adia}, can serve as useful lower and upper estimates of f_{rigid} in the intermediate regime. This is illustrated again in Figure 9 which shows plots

of $f_{\text{rigid}}^{\text{sudd}}$ defined in section 5 and $f_{\text{rigid}}^{\text{adia}}$ found from the adiabatic channel (AC) approach.[8,15,22] The rather narrow range between $f_{\text{rigid}}^{\text{sudd}}$ and $f_{\text{rigid}}^{\text{adia}}$ reflects the only weak effect of rotationally inelastic events on the way to the formation of the complex. The question, whether the same persists in quantum capture, i.e., whether the rate coefficients can be usefully bracketed, on the one hand, between those presented in this paper for sudden capture and, on the other hand, for the adiabatic capture such as described by the standard AC approach, needs to be elaborated in the future.

Acknowledgment. The authors thank Professor V. Aquilanti for numerous stimulating discussions. Finally, financial support of this work by the European Office for Aerospace Research and Development (Grant No. FA 8655-09-1-3001) is also acknowledged.

References and Notes

(1) Landau, L.; Lifshitz, E. *Classical Mechanics*; Pergamon Press: Oxford, U.K., 1976.

(2) Landau, L.; Lifshitz, E. *Quantum Mechanics (Non-Relativistic Theory)*; Pergamon Press: Oxford, U.K., 1977.

(3) Rackham, E. J.; Huarte-Larranaga, F.; Manolopoulos, D. E. *Chem. Phys. Lett.* **2001**, *343*, 356.

(4) Rackham, E. J.; Gonzalez-Lezaña, T.; Manolopoulos, D. E. *J. Chem. Phys.* **2003**, *119*, 12895.

(5) Alexander, M. H.; Rackham, E. J.; Manolopoulos, D. E. *J. Chem. Phys.* **2004**, *121*, 5221.

(6) Atahan, S.; Alexander, M. H.; Rackham, E. J. *J. Chem. Phys.* **2005**, *123*, 204306.

(7) Su, T.; Chesnavich, W. J. *J. Chem. Phys.* **1982**, *76*, 5183.

(8) Maergoiz, A. I.; Nikitin, E. E.; Troe, J.; Ushakov, V. G. *J. Chem. Phys.* **1996**, *105*, 6263.

(9) Dashevskaya, E. I.; Maergoiz, A. I.; Ushakov, V. G. *Z. Phys. Chem.* **2002**, *216*, 605.

(10) Fabrikant, I. I.; Hotop, H. *Phys. Rev. A* **2001**, *63*, 022706.

(11) Klar, D.; Ruf, M.-W.; Fabrikant, I. I.; Hotop, H. *J. Phys. B: At. Mol. Opt. Phys.* **2001**, *34*, 3855.

(12) Dashevskaya, E. I.; Litvin, I.; Nikitin, E. E.; Troe, J. *Phys. Chem. Chem. Phys.* **2008**, *10*, 1270.

(13) Dashevskaya, E. I.; Litvin, I.; Maergoiz, A. I.; Nikitin, E. E.; Troe, J. *J. Chem. Phys.* **2003**, *118*, 7313.

(14) Takayanagi, K. *J. Phys. Soc. Jpn.* **1978**, *45*, 976.

(15) Troe, J. *J. Chem. Phys.* **1987**, *87*, 2773.

(16) Maergoiz, A. I.; Troe, J. *J. Chem. Phys.* **1993**, *99*, 3218.

(17) Maergoiz, A. I.; Troe, J.; Weiss, Ch. *J. Chem. Phys.* **1994**, *101*, 1885.

(18) Bethe, H. A. *Rev. Mod. Phys.* **1937**, *9*, 69.

(19) Wigner, E. P. *Phys. Rev.* **1948**, *73*, 1002.

(20) Stoecklin, T.; Clary, C. *J. Chem Soc., Faraday Trans.* **1992**, *88*, 901.

(21) Troe, J. *Z. Phys. Chem.* **1989**, *NF 161*, 209.

(22) Troe, J. *J. Chem. Phys.* **1996**, *105*, 6249.

(23) Troe, J. *Ber. Bunsen-Ges. Phys. Chem.* **1997**, *101*, 438.

(24) Troe, J. *J. Chem. Soc., Faraday Trans.* **1997**, *93*, 885.

(25) Troe, J. *Z. Phys. Chem.* **2004**, *218*, 457.

JP901515E